

# Enhanced thermal stability and broadened Raman scattering of tellurite glasses by co-doping heavy metal oxides

Q. YANG, Q. QIAN, D. D. CHEN, Q. Y. ZHANG\*, Z. H. JIANG

MOE Key laboratory of Specially Functional Materials and Institute of Optical Communication Materials, South of China University of Technology Guangzhou 510640, China

Tungsten-niobium-tellurite (TNT) glasses and molybdenum-niobium-tellurite (MNT) glasses have been investigated for their potential application in broadband Raman fiber amplifier. Effects of the addition of heavy metal oxides (HMO) (HMO=Nb<sub>2</sub>O<sub>5</sub>, WO<sub>3</sub>, or MoO<sub>3</sub>) on the thermal stability against crystallization and Raman spectral properties of tellurite glasses have been discussed. The results suggest that the addition of HMO could largely improve the thermal stabilities of tellurite glasses. Moreover, TNT and MNT glasses exhibit strong Raman peaks at around 848 and 915 cm<sup>-1</sup>. It is noted that the mid-high frequency Raman region of the tellurite glass by co-doping HMO expand from 550 to 1000 cm<sup>-1</sup> with the maximum full width at half maximum (FWHM) of about 375 cm<sup>-1</sup>, indicating TNT and MNT glasses are promising host-materials for broadband Raman fiber amplification.

(Received May 18, 2009; accepted June 15, 2009)

*Keywords:* Tellurite glass, Thermal stability, Raman spectroscopy, Raman amplifier, Heavy metal oxides

## 1. Introduction

To meet the current requirement of the optical telecommunication and other data transmitting services, it is required to improve the transmission capacity of wavelength division multiplexing (WDM) system. Optical amplifier is a key device which impacts the communication bands and transmission distance in the whole transmission system. Compared to the conventional C-band (1530-1565 nm), which is supported by Er-doped fiber amplifier (EDFA), Raman fiber amplifier (RFA) offers a valuable solution to extend the use of communication windows in WDM systems. RFA is an amplifier based on transmission fiber, which has lots of excellent features as follows: a broad amplification bandwidth, flexible amplification region by changing the excitation wavelength, and gain flattening by multi-wavelength excitation [1]. Silica glass has been widely used in fiber Raman amplifiers due to its low loss. However, the primary disadvantages of fused silica are its limited Raman gain and bandwidth. Tellurite glasses, however, have received much attention because of their high Raman scattering coefficient. Tellurite glasses have shown a broad Raman scattering band due to the several peaks at ~440, 660 and 740 cm<sup>-1</sup> [2-5]. And it is possible to modify the tellurite network and broaden the Raman scattering bandwidth [2] by adding heavy metal oxides (HMO), such as Nb<sub>2</sub>O<sub>5</sub>, Bi<sub>2</sub>O<sub>3</sub>, WO<sub>3</sub>, MoO<sub>3</sub>, Ta<sub>2</sub>O<sub>5</sub> and

Tl<sub>2</sub>O.

Herein, the main objective of this work is to carry out a detailed study on effects of HMO (HMO=Nb<sub>2</sub>O<sub>5</sub>, WO<sub>3</sub>, or MoO<sub>3</sub>) contents on the thermal stabilities and Raman scattering properties of tungsten-niobium-tellurite (TNT) glasses and molybdenum-niobium-tellurite (MNT) glasses, to examine their suitability as potential optical glasses for RFA.

## 2. Experimental

### 2.1 Glass preparation

TNT glasses with molar compositions of (75-x)TeO<sub>2</sub>-10ZnO-5Na<sub>2</sub>O-10Nb<sub>2</sub>O<sub>5</sub>-xWO<sub>3</sub> (x=0, 5, 10 and 15, namely TNT0, TNT5, TNT10 and TNT15, respectively), and MNT glasses with molar compositions of (75-x)TeO<sub>2</sub>-10ZnO-5Na<sub>2</sub>O-10Nb<sub>2</sub>O<sub>5</sub>-xMoO<sub>3</sub> (x=5, 10 and 15, namely MNT5, MNT10 and MNT15, respectively) were fabricated by using reagent-grade TeO<sub>2</sub>, ZnO, Na<sub>2</sub>CO<sub>3</sub>, Nb<sub>2</sub>O<sub>5</sub>, WO<sub>3</sub>, MoO<sub>3</sub> as the starting materials. Appropriate amounts of chemicals (20-30 g) were mixed well and melt in a platinum crucible at 900 °C for 30 min. After annealing, samples for optical and spectral properties measurements were cut into rectangular 30×20×2 mm<sup>3</sup> shapes and optically polished.

## 2.2 Measurements

The densities of glasses were determined according to the Archimedes' principle using the distilled water as the medium. The refractive indices of the samples were recorded on a Metricon 2010 by means of a prism coupling method at 632.8 nm. Thermal analysis of tellurite glasses were examined by using a Netzsch STA 449C Jupiter different scanning calorimeter (DSC) at a heating rate of 10 °C/min from 25 ° to 700 °C.

The micro-Raman scattering spectra were recorded by a Raman spectrometer (RM2000) in the range of 200-1200  $\text{cm}^{-1}$  in backscattering geometry. The samples were excited using 20 mW lasers of 514.5 nm wavelengths. All the measurements were carried out at room temperature.

## 3. Results and discussion

### 3.1 Thermal and physical properties of glasses

Table 1 summarizes the values of density ( $\rho$ ), refractive index ( $n$ ) for TNT and MNT tellurite glasses. It is found that both the density and refractive index of the glasses increase monotonically with increasing HMO contents.

The difference between the glass transition temperature ( $T_g$ ) and the onset crystallization temperature ( $T_x$ ),  $\Delta T = T_x - T_g$ , which represents the temperature interval during the nucleation taking place, has been frequently used as an approximate estimation of glass formation ability or glass thermal stability. To avoid any crystallization during fiber drawing, it is desirable for a glass host to have a  $\Delta T$  as large as possible. It is believed that a large  $\Delta T$  above 100 ° is desirable for low-loss fiber fabrication [6].

The DTA curves obtained from all samples are shown in Figs. 1 and 2. Meanwhile, the values of  $T_g$ ,  $T_x$  and  $\Delta T = T_x - T_g$  of the glasses are also listed in Table 1.

Table 1. Density, refractive indices and thermal properties of tellurite glasses.

Sample	Refractive indices	$T_g$ (°C)	$T_x$ (°C)	$\Delta T$ (°C)	Density ( $\text{g}/\text{cm}^3$ )
TNT0	2.1104	359	468	109	5.34
TNT5	2.1156	355	484	129	5.47
TNT10	2.1201	361	499	138	5.59
TNT15	2.1247	371	512	141	5.67
MNT5	2.0811	361	487	126	5.40
MNT10	2.0885	365	495	130	5.48
MNT15	2.0932	367	509	142	5.56

From Fig. 1, with increasing HMO contents, no significant increase in the  $T_g$  was observed. However,  $T_x$  increased consistently when  $\text{TeO}_2$  was subsequently

replaced by HMO.

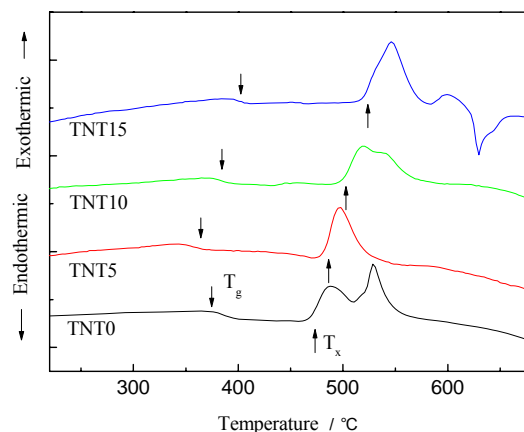


Fig. 1. DTA curves of TNT0, TNT5, TNT10 and TNT15 glasses.

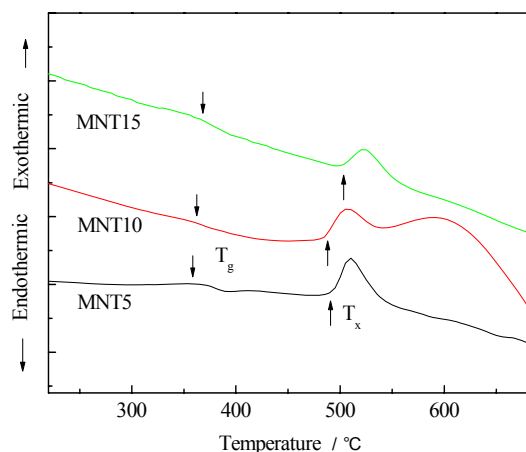


Fig. 2. DTA curves of MNT5, MNT10 and MNT15 glasses.

All the glasses in the Table 1 have  $\Delta T$  values above 100 °C, and this value of TNT15 and MNT15 glasses is more than 140 °C, indicating that these glasses possess high thermal stabilities and are desirable for low-loss fiber fabrication.

### 3.2 Raman spectra of tellurite glasses

Fig. 3 shows the spontaneous Raman scattering spectra of TNT glasses containing  $\text{WO}_3$  from 0 to 15 mol%. The inset of Fig. 3 is the full width at half maximum (FWHM) of the glasses with the change of  $\text{WO}_3$  content. All the samples studied here were measured at identical condition. It can observe clearly that Raman spectra of all glasses in the investigations

show major bands in the low frequency region 200-540  $\text{cm}^{-1}$ , mid-frequency region 540-875  $\text{cm}^{-1}$  and high frequency region 875-1100  $\text{cm}^{-1}$ .

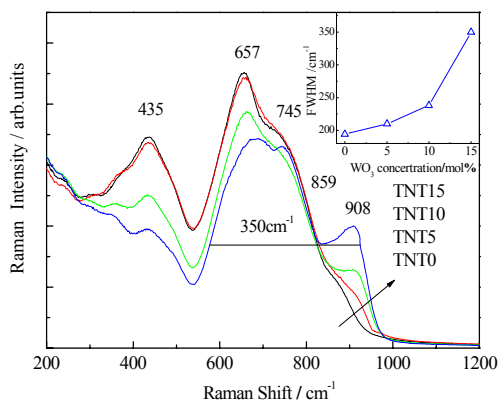


Fig. 3. Raman spectra of TNT0, TNT5, TNT10 and TNT15 glasses, the inset shows the Raman bandwidths of the glasses with the increase in  $\text{WO}_3$  content.

The peak centered at the low frequency region 435  $\text{cm}^{-1}$  is ascribed to the symmetrical stretching or bending vibrations of Te-O-Te linkages. The peak centered at the mid-frequency region 657 is ascribed to the antisymmetric stretching vibrations of Te-O-Te linkages by two unequivalent Te-O bonds containing bridging oxygens (BO) in  $\text{TeO}_4$  trigonal bipyramid (tbp), and the peak centered at 745  $\text{cm}^{-1}$  is ascribed the symmetrical stretching vibrations of Te-O and Te=O bonds containing nonbridging oxygens (NBO) in  $\text{TeO}_3$  trigonal pyramid (tp) and  $\text{TeO}_{3+1}$  polyhedra. All the peaks above mentioned are identified with the network structure of tellurite glasses. In addition, all the samples also show peaks at the high frequency region 859 and 908  $\text{cm}^{-1}$  and the Raman spectrum expand to the high frequency region  $\sim 950 \text{ cm}^{-1}$ . The two peaks are attributed to the vibration of Nb and its neighboring nonbridging oxygens in  $\text{NbO}_6$  octahedra and the vibrations of W-O and W=O bonds in  $\text{WO}_4$  tetrahedra [7], respectively.

With the addition of  $\text{Nb}_2\text{O}_5$  and  $\text{WO}_3$ , the Raman spectral shape of TNT glasses is changed gradually. With increasing  $\text{Nb}_2\text{O}_5$  and  $\text{WO}_3$  contents, the relative intensities of peaks at 435 and 657  $\text{cm}^{-1}$  decrease while the relative intensity of the peak at 745  $\text{cm}^{-1}$  increases, indicating the transformation of  $\text{TeO}_4$  tbp into  $\text{TeO}_3$  tp and  $\text{TeO}_{3+1}$ . There are two significant reasons for the change. Firstly, with substituting  $\text{TeO}_2$  by  $\text{Nb}_2\text{O}_5$  and  $\text{WO}_3$ , the relative contents of ZnO and  $\text{Na}_2\text{O}$  increase in glasses. ZnO and  $\text{Na}_2\text{O}$ , as network modifiers which break the tellurite glasses network, are known to contribute to the formation of  $\text{TeO}_3$  and  $\text{TeO}_{3+1}$  structural unites in the glass [8,9]. Secondly, with the addition of  $\text{WO}_3$  it would be expect that the tellurite glass network is depolymerised [10]. When  $\text{WO}_3$  is added in tellurite glass

as glass network modifiers, the original network structures are broken and  $\text{WO}_3$  cleaved a Te-O bond in the basic  $\text{TeO}_4$  substructure and transformed this into  $\text{TeO}_3$  and  $\text{TeO}_{3+1}$  structural unites. With these two processes, Te-O-Te linkages depolymerize gradually, providing plenty of free oxygens, and the number of bridging oxygens decreases, causing the transformation of  $\text{TeO}_4$  tbp into  $\text{TeO}_3$  tp with more NBO atoms via the intermediate coordination of  $\text{TeO}_{3+1}$  [11,12]. In other words, the changing of the intensities of the peaks at around 435, 657 and 740  $\text{cm}^{-1}$  can be attributed to the transformation of  $\text{TeO}_4$  tbp into  $\text{TeO}_3$  tp via the intermediate coordination of  $\text{TeO}_{3+1}$  with the increasing of  $\text{Nb}_2\text{O}_5$  and  $\text{WO}_3$  contents.

Addition of  $\text{WO}_3$  and  $\text{Nb}_2\text{O}_5$  change the shape of the Raman spectrum from the one in which  $\text{TeO}_4$  tbp is the major contributor to the ones in which  $\text{TeO}_3$  tp and  $\text{TeO}_{3+1}$  polyhedra are the major contributors. The FWHM of the glasses increases gradually with increasing  $\text{Nb}_2\text{O}_5$  and  $\text{WO}_3$  contents. Raman spectral bandwidth at FWHM increases from  $\sim 209 \text{ cm}^{-1}$  to  $\sim 355 \text{ cm}^{-1}$  as the  $\text{WO}_3$  content increased from 0 to 15 mol%, which has obviously improved the Raman scattering bandwidth compared to the case of silica glasses. However, the peak at 908  $\text{cm}^{-1}$  have risen solely and as a result it does not overlap with the third Raman scattering peak of the tellurite glass centered at 745  $\text{cm}^{-1}$ . This is practically not desirable as it would produce a seam between the two Raman scattering peaks on the spectrum.

$\text{MoO}_3$  has been added to the tellurite glasses in the same manner and Fig. 4 shows the spontaneous Raman scattering spectra of the MNT glasses containing  $\text{MO}_3$  from 5 to 15 mol%, as well as FWHM of the glasses with the change of  $\text{MoO}_3$  content are shown in the inset of Fig. 4.

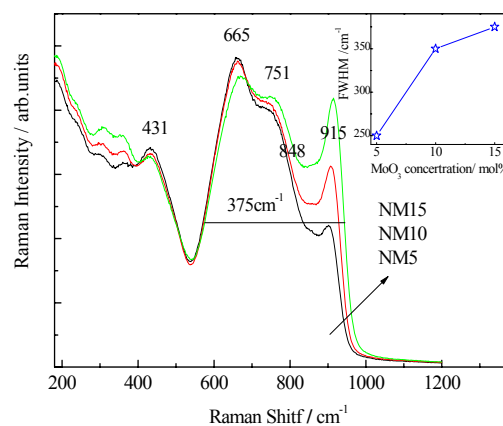


Fig. 4. Raman spectra of MNT5, MNT10 and MNT15 glasses, the inset shows the Raman bandwidths of the glasses with the increase in  $\text{MO}_3$  content.

All three glasses exhibit the peaks at around 431, 665, and 751  $\text{cm}^{-1}$ , which are corresponding to the same structural units with the peaks in Fig. 3. In addition, the presence of  $\text{MoO}_3$  in the glass is revealed by a Raman peak at around 915  $\text{cm}^{-1}$  due to Mo=O vibrations in  $\text{MoO}_6$  octahedra [13].

With the amount of  $\text{MO}_3$  increasing, the bandwidths at FWHM of the glasses enhance drastically. Addition of  $\text{WO}_3$  and  $\text{MoO}_3$  make the Raman spectra exhibit similar characteristic Raman scattering peaks at around 900-920  $\text{cm}^{-1}$ . Unlike to the case of TNT glass, it is significant for the glass with  $\text{MoO}_3$  that the peak centered at 848  $\text{cm}^{-1}$  is effectively bridging the peaks centered at 915  $\text{cm}^{-1}$  and 751  $\text{cm}^{-1}$  because the peaks centered at 915 and 848  $\text{cm}^{-1}$  overlap with the peaks centered at 665  $\text{cm}^{-1}$  and 751  $\text{cm}^{-1}$  corresponding to the tellurite glass network. The Raman spectrum expands from the mid-frequency region 550  $\text{cm}^{-1}$  to the high frequency region 1000  $\text{cm}^{-1}$ . Raman spectrum bandwidth at FWHM increases from  $\sim 250 \text{ cm}^{-1}$  to  $\sim 375 \text{ cm}^{-1}$  as the  $\text{MO}_3$  content increased from 0 to 15mol%, which is near 80% higher than that of silica glasses ( $\sim 210 \text{ cm}^{-1}$ ).

#### 4. Conclusions

In summary, we reports on effects of the addition of heavy metal oxides (HMO) ( $\text{HMO}=\text{Nb}_2\text{O}_5$ ,  $\text{WO}_3$ , or  $\text{MoO}_3$ ) on the thermal stability against crystallization and Raman spectral properties of tellurite glasses. The results suggest that the addition of HMO could largely improve the thermal stabilities of tellurite glasses. Moreover, TNT and MNT glasses exhibit strong Raman peaks at around 848 and 915  $\text{cm}^{-1}$ . The mid-high frequency Raman region of the tellurite glass by co-doping HMO expand from 550 to 1000  $\text{cm}^{-1}$  with FWHM of about 375  $\text{cm}^{-1}$ . Our results indicate that TNT and MNT glasses are promising candidates for broadband Raman fiber amplification.

#### Acknowledgements

This work was supported by the National Natural Science Foundation of China (No. 50602017).

#### References

- [1] A. Mori, H. Masuda, K. Shikano, M. Shimizu, J. Lightwave Technol. **21**, 1300 (2003).
- [2] G. S. Murugan, T. Suzuki, Y. Ohishi, Appl. Phys. Lett. **86**, 161109 (2005).
- [3] A. Mori, H. Masuda, K. Shikano, K. Oikawa, K. Kato, M. Shimizu, Electron. Lett. **37**, 24 (2001).
- [4] H. Masuda, A. Mori, K. Shikano, K. Oikawa, K. Kato, M. Shimizu, Electron. Lett. **38**, 16 (2002).
- [5] H. Masuda, A. Mori, K. Shikano, M. Shimizu, J. Lightwave Technol. **24**, 504 (2006).
- [6] J. S. Wang, E. M. Vogel, E. Snitzer, Opt. Mater. **3**, 187 (1994).
- [7] I. Shaltout, Y. Tang, R. Braunstein, A. M. Abuelazm, J. Phys. Chem. Solids **56**, 141 (1995).
- [8] T. Sekiya, N. Mochida, A. Ohtsuka, J. Non-Cryst. Solids **144**, 128 (1992).
- [9] W. J. Chung, B. J. Park, H. S. Seo, J. T. Ahn, Y. G. Choi, Chem. Phys. Lett. **400**, 419 (2006).
- [10] M. D. O'Donnell, K. Richardson, R. Stolen, C. Rivero, T. Cardinal, M. Couzi, D. Furniss, A. B. Seddon, Opt. Mater. **10**, 1061 (2007).
- [11] P. Charton, P. Thomas, P. Armand, J. Non-Cryst. Solids **321**, 81 (2003).
- [12] V. Nazabal, S. Todoroki, A. Nukui, T. Matsumoto, S. Suehara, T. Hondo, T. Araki, S. Inoue, C. Rivero, T. Cardinal, J. Non-Cryst. Solids **325**, 85 (2003).
- [13] T. Sekiya, N. Mochida, S. Ogawa, J. Non-Cryst. Solids **185**, 135 (1995).

\*Corresponding author: qyzhang@scut.edu.cn